

Hubble Space Telescope Observations of the Gravitationally Lensed Cloverleaf Broad Absorption Line QSO H1413+1143: Imaging Polarimetry and Evidence for Microlensing of a Scattering Region¹

Kyu-Hyun Chae,^{2,3,4} David A. Turnshek,^{2,3} Regina E. Schulte-Ladbeck,^{2,3}

Sandhya M. Rao,^{2,3} and Olivia L. Lupie^{2,5}

Received _____; accepted _____

¹Based on observations made with the NASA/ESA *Hubble Space Telescope*, obtained from the Space Telescope Science Institute, which is operated under NASA contract NAS 5-26555.

²email: chae@jb.man.ac.uk, turnshek@pitt.edu, rsl@pitt.edu, rao@phyast.pitt.edu, lupie@stsci.edu

³Dept. of Physics & Astronomy, University of Pittsburgh, Pittsburgh, PA 15260, USA

⁴Present address: University of Manchester, JBO, Macclesfield, Cheshire SK11 9DL, UK

⁵Space Telescope Science Institute, 3700 San Martin Drive, Baltimore, MD 21218, USA

ABSTRACT

We report the results of *Hubble Space Telescope* Wide Field and Planetary Camera 2 broadband F555W and F702W photometric and F555W polarimetric observations of the “Cloverleaf” QSO H1413+1143. This is a four-component gravitationally-lensed broad absorption line (BAL) QSO. Observations were obtained at two epochs in March 1999 and June 1999 separated by ≈ 100 days. The observations were photometrically and polarimetrically calibrated using the standard “pipeline” calibration procedures implemented at the Space Telescope Science Institute. The goal of our program was to detect any *relative* changes among the components and between the two epochs. Over this time baseline we detected an ≈ 0.07 mag dimming in component D of the lensed image, which we interpret as evidence for microlensing. In March 1999 we find significant evidence for a difference in the relative linear polarization of component D in comparison to the other three components; in June 1999 the combined polarization of the Cloverleaf components was lower. In March 1999 the apparently microlensed component D has a rotated polarization position angle and a somewhat higher degree of polarization than the other three components. We suggest that this difference in polarization is due to microlensing magnification of part of a scattered-light (i.e. polarized) continuum-producing region. The results indicate that in the Cloverleaf the size-scale of the polarized scattered-light region exceeds $\approx 10^{16}$ cm but lies interior to the region producing the broad emission lines ($< 10^{18}$ cm).

Subject headings: polarization — techniques: polarimetric — quasars: individual (H1413+1143, Cloverleaf) — quasars: structure — gravitational lensing

1. Introduction

Broad absorption line (BAL) QSOs comprise $\approx 10\%$ of the objects in optically selected QSO samples. Their defining characteristics are deep, high-velocity (usually $< 0.1c$) absorption troughs blueward of high-ionization broad emission lines (BELs) in species such as Si IV, C IV, N V, and O VI (e.g. Turnshek 1988 and Weymann et al. 1991). They also have a distribution of linear polarizations which peaks at a significantly higher polarization in comparison to non-BAL radio-quiet QSOs (Schmidt & Hines 1999; Hutsemékers, Lamy & Remy 1998; Goodrich 1997; Turnshek 1988); indeed the origin of much of the polarization in most non-BAL QSOs is probably the Galactic interstellar medium.

The observed polarization properties of BAL QSOs depend on, and therefore contain relevant astrophysical information on, the geometries and physical properties of the inner regions of these QSOs (i.e. the narrow emission-line region, the dusty torus, the BAL region, the BEL region, any scattering regions, the thermal accretion disk, and any region producing non-thermal emission). Recent studies on the polarization properties of BAL QSOs (Schmidt & Hines 1999; Hutsemékers et al. 1998; Ogle 1998; Goodrich 1997) have shown that: (1) their continuum polarizations are, on average, significantly higher than non-BAL radio-quiet QSOs, with the degree of polarization rising mildly toward shorter wavelengths, (2) the BALs are more highly polarized than the continuum, with position angle rotations observed in the BAL troughs, (3) BELs in *some* BAL QSO spectra are polarized, but the degree of polarization is lower than in the continuum and the polarization position angles are not necessarily similar, and (4) there is some evidence that the degree of polarization is positively correlated with the BAL QSO’s balnicity index (defined by Weymann et al. 1991) and the presence of low-ionization BALs, with objects having higher balnicity indices and/or low-ionization BALs being more polarized on average.

While it is generally agreed that the scattered continuum is, in large part (if not

totally), responsible for the observed net polarizations observed in BAL QSOs (e.g. Goodrich & Miller 1995; Ogle 1998; Schmidt & Hines 1999), the size-scales and geometries of the regions containing scattering particles (i.e. electrons and/or dust particles) are not yet well constrained. However, the gravitationally-lensed Cloverleaf BAL QSO H1413+1143 ($z_{em} \approx 2.55$) is at present a unique laboratory for study of the polarization mechanism. Its four components are known to have a combined net continuum polarization which has varied between 1.5 – 3.5% over a decade (Goodrich & Miller 1995) and one of the four components (component D) shows evidence for microlensing in the form of light variability (see Angonin et al. 1990, Arnould et al. 1993, Remy et al. 1996, Ostensen et al. 1997, and new evidence presented here) and differences in BEL and BAL profile characteristics (Chae & Turnshek 1999 and references therein).

We know that, in principle, microlensing could alter the net polarization of a single gravitationally-lensed component, since this process selectively produces additional magnification of a small region of an Einstein ring radius on the source plane. The resulting polarization properties during microlensing would depend on the detailed geometry of the region where the polarized light originates (see Belle & Lewis 2000 for examples). Consequently, the observed component polarization properties during microlensing can be used to constrain the projected sizes of the scattering regions and their projected distances from any central black hole (i.e. the central region of the accretion disk).

In this *Letter*, we report the results of *Hubble Space Telescope (HST)* Wide Field and Planetary Camera 2 (WFPC2) broadband F555W and F702W photometric and F555W polarimetric observations of the Cloverleaf. We find new evidence for microlensing of component D and show that component D has significantly different relative polarization properties than the other three components. In §2 we describe our observations and data analysis; in §3 we present the results; and in §4 we discuss the implications for models of

the production of polarized light in BAL QSOs. We note that this paper is the fifth in a series of *HST* results on the Cloverleaf by members of our group. Earlier results include constraints on the sizes and shapes of absorbing regions producing the BALs (Turnshek 1995), constraints on the component image locations and magnifications (Turnshek et al. 1997), constraints on the properties of the intervening absorbers seen in the component spectra (Monier, Turnshek & Lupie 1998), and implications for gravitational-lens models of the Cloverleaf, including a constraint on BEL region size scales (Chae & Turnshek 1999).

2. Observations and Data Analysis

For this study the Cloverleaf QSO was observed at two closely-spaced epochs, 15-16 March 1999 and 23-24 June 1999. Broadband F555W filter observations were made with the Wide Field Camera 2 (WFC2) with either no polarizer or one of four polarizers (POLQ, POLQN18, POLQN33, POLQP15). Also, F702W filter observations were made with the Planetary Camera 2 (PC2) and no polarizer. The observations are summarized in Table 1 and numbered as a referencing convenience. Each F555W observation consisted of taking two sets of four dithered images. The pixel position of component A in the second set was chosen to coincide with that of component D in the first set. In addition to the normal procedures for identifying cosmic ray contamination of WFPC2 images, all pipeline processed images were also individually examined. Cosmic rays present near the Cloverleaf components were removed interactively and the data were replaced using interpolation. After sky subtraction, each set of images was combined via the variable-pixel linear reconstruction algorithm, or the “drizzling” algorithm (Fruchter & Hook 1998; Fruchter et al. 1997). Point spread function (PSF)-fitting photometry showed that the photometric results of the two sets for each observation were consistent with each other. Finally, all eight images in the two sets were drizzled to form one image. The procedure of taking dithered

images and combining them via drizzling partially restores the PSF, thereby facilitating more accurate PSF-fitting photometry. Using the final drizzled image for each observation, an empirical PSF was constructed iteratively from the Cloverleaf components themselves, and then the Cloverleaf components were fitted simultaneously using this empirical PSF.⁶ For the above procedures, the Image Reduction and Analysis Facility (IRAF) packages DAOPHOT and STSDAS were used. The reliability of the above PSF-fitting photometry was tested by visually examining the PSF-subtracted region and computing pixel statistics within the subtracted region; the mean pixel data number (DN) value within the region was $|\overline{DN}| \lesssim 0.1\sigma$ in all cases.

The observations were photometrically and polarimetrically calibrated using the standard “pipeline” calibration procedures implemented at the Space Telescope Science Institute. The goal of our program was not to make absolute measurements, but to detect any relative changes among the components and between the two epochs. Thus, the errors we quote based on our differencing procedures are statistical in nature. Our relative measurements and the resulting interpretation should not be affected by a small systematic error in the pipeline calibration.

The derived F555W photometric results without polarizers (i.e. observation numbers 1, 2, 3 and 11, 12, 13) were found to be highly consistent with one another. This served as an independent test, confirming the reliability of our method of photometry. The F702W photometric observations without polarizers (i.e. observation numbers 4, 5, 6 and 16, 17,

⁶We could not use the “Tiny TIM” software to generate PSFs since it does not have the capability of incorporating the effects of the polarizing filters. We found that all individual images taken with the POLQN33 polarizer (for both epochs) and the POLQP15 polarizer (for the March epoch) had substantially modified PSFs in terms of FWHM and peak pixel value in comparison to images taken without polarizers.

18) allowed us to fill up the remaining time available for exposures in a number of the orbits using a filter that had previously been used to observe the Cloverleaf, but without the goal of deriving photometry using drizzling. We found the statistical errors to be considerably reduced using the drizzling method.

In order to determine the Stokes parameters (I, Q, U), the F555W observations with polarizers were incorporated into the WFPC2 polarization calibration model (Biretta & McMaster 1997). The Stokes parameters are related to the degree of polarization (p) and the position angle (PA) via the relations $p = (u^2 + q^2)^{1/2}$ and $PA = (1/2) \tan^{-1}(u/q) + n\pi/2$ where $q \equiv Q/I$, $u \equiv U/I$, and $n = 0, 1, 2$ for $u \geq 0$ and $q \geq 0$, $u \geq 0$ and $q \leq 0$ (or, $u < 0$ and $q < 0$), and $u \leq 0$ and $q \geq 0$, respectively. For the March epoch, six observations were incorporated simultaneously using a χ^2 fitting technique to determine the Stokes parameters.⁷ The χ^2 is defined by

$$\chi^2 = \sum_i \left(\frac{C_i^{\text{obs}} - C_i^{\text{mod}}(I, Q, U)}{\sigma_i} \right)^2, \quad (1)$$

where $i = 7, 8, 9, 10, 11, 12$ are the March observation numbers, C_i^{obs} and C_i^{mod} are the observed and calibration-model-predicted counts, respectively, and σ_i are the statistical errors in the observed counts. The minimum χ^2 value was $\chi_{\text{min}}^2 < 7$, with 3 degrees of freedom for all components, indicating that there is a reasonable match between the model and the data. The 1σ statistical errors for each Stokes parameter were estimated using $\Delta\chi^2 = \chi^2 - \chi_{\text{min}}^2 = 1$ (e.g. Press et al. 1992), and the statistical errors for p and PA

⁷For the March data we did not use the web-based WFPC2 polarization calibration tool or the IRAF *IMPOL* package, since the former can take only three relative counts at one time while the latter takes the images themselves as input using only aperture photometry, which is less accurate for the “crowded” Cloverleaf field. It was possible to use the web-based WFPC2 polarization calibration tool for the June data.

were estimated assuming Gaussian error propagation. For the June epoch ($i = 19, 20, 21$), the Stokes parameters were determined by solving $C_i^{\text{obs}} = C_i^{\text{mod}}(I, Q, U)$ for I , Q and U ,⁵ with the statistical errors for the Stokes parameters being estimated using Gaussian error propagation of the photometric errors via these equations.

The results for the June epoch are much less reliable in comparison to the March results. There are two reasons for this. First, the June measurements were made at only three polarization angles, while the March measurements were made at six polarization angles. Second, according to the pipeline calibration, the degree of polarization is evidently smaller in June 1999, which gives rise to a lower signal-to-noise ratio for a fixed photometric error. Thus, the June results should not be given high weight. Since the March data show the polarization of components A, B and C to be similar, for the June epoch we report only the results for the combined measured polarization of components A, B and C, and we report the measured polarization of component D separately.

3. Results

Below we consider the results of our WFPC2 observations in two separate parts. First, we consider any evidence for photometric variations among the four lensed components of the Cloverleaf between the June 1999 and March 1999 epochs (§3.1, Table 2a,b). Second, we consider any evidence for differences in the linear polarization among the four lensed components (§3.2, Table 3).

3.1. Brightness Variation of Component D: Evidence for Microlensing

The photometric observations of the Cloverleaf without polarizers were used to search for and measure any brightness variations over the time baseline (≈ 100 days)

which separated the two epochs of observation. As noted earlier, the individual F555W photometric results for each epoch were very consistent with one another; the average F555W photometric results for each epoch are reported in Table 2a,b. The average F702W photometric observations are also reported in Table 2a,b, but are less accurate. The photometric results are shown in Figure 1. They clearly indicate that component D decreased its brightness over the ≈ 100 day time baseline, while the other three components either remained about the same brightness (i.e. components B and C) or slightly increased their brightness (i.e. component A). Assuming an insignificant wavelength dependence to the brightness variation over the F555W and F702W passbands, using variance-weighting we find $\Delta m_D = 0.074 \pm 0.004$ mag and $\Delta m_A = -0.023 \pm 0.004$ mag. Evidence for brightness variations in components B and C are at the 2σ level of significance or less.

Recent detailed work on modeling the Cloverleaf lens and time delays (Chae & Turnshek 1999) suggests that in all reasonable models component C is the leading component and component D is the trailing component, with the maximum time delay being model-dependent and lying in the range $\approx 7 - 41$ days. However, the predicted time delays between components C and A or components C and B are always a significant fraction (at least $\approx 30\%$) of the predicted time delay between components C and D. Given these lens models and observations of brightness variations in other BAL QSOs (Sirola et al. 1997), we believe that these new photometric data on the Cloverleaf are not likely to be consistent with simply an intrinsic variation in the source BAL QSO’s brightness coupled with time delays among the four components. The most likely cause of the light variation of component D is microlensing, which is consistent with the findings of others who have studied brightness variations in the Cloverleaf (Angonin et al. 1990; Arnould et al. 1993; Remy et al. 1996; Ostensen et al. 1997).

3.2. Polarimetric Results

For the March 1999 and June 1999 epochs of observation, Table 3 gives the measured normalized Stokes parameters q and u , the degree of linear polarization (p), the corrected degree of linear polarization (p_{corr}) which takes into account the bias toward measuring higher polarization in low signal-to-noise data (Wardle & Kronberg 1974), and the polarization position angle (PA). For the March observations the derived q and u Stokes parameters are shown in Figure 2, and it is seen that the polarizations of components A, B and C differ from the polarization of component D.

The main points of the polarimetric results are: (1) The polarizations of components A, B, and C in March 1999 have no appreciable differences. (2) As is clearly seen in Figure 2, in March 1999 component D has a significantly different relative polarization in comparison to the other three components. The *relative* normalized Stokes parameters between component D and the combination of the other components in March 1999 is $\Delta q_{\text{D},\overline{\text{ABC}}} = -1.26 \pm 0.54\%$ and $\Delta u_{\text{D},\overline{\text{ABC}}} = -2.32 \pm 0.61\%$ (Table 3), which is a difference in polarization at a level of significance of 4.5σ . (3) The pipeline calibrated data suggest that the net polarization of the Cloverleaf changed between the March 1999 and June 1999 epochs, with the polarization being smaller during the June epoch.

4. Discussion

These results are the first observational ones which address resolved polarization measurements in a gravitationally-lensed QSO and, owing to our interpretation (§3.1 and below), the first to report evidence for microlensing of a polarized-light region in a QSO.

Before we examine the implications of our interpretation, we should comment on some issues which can affect the interpretation. For example, polarization induced by any dust

which is present along the sight-line toward the Cloverleaf is unlikely to be responsible for the added component of polarization that appears to be present in component D.⁸ There are several reasons for this. First, multicolor (F336W, F702W, F814W) *HST* WFPC2 observations have shown that differential dust reddening is, in fact, present across the Cloverleaf components. Component B is the most reddened and component C is the least reddened, with the F336W–F814W color index being 0.56 ± 0.04 mag between components B and C. The reddening of components A and D are intermediate (see figure 3 in Turnshek et al. 1997). The source of this differential reddening may be dust in the interstellar medium of the lensing galaxy. However, since interstellar polarization is normally proportional to the amount of reddening, we would not expect the change in polarization of component D to be related to the reddening. Second, if the source of the polarization was the lens, it would seem unlikely that the induced polarization would be different only for component D. Third, interstellar polarization would not be expected to be time-variable, but the observations indicate that the polarization changed between the March 1999 and June 1999 epochs. Fourth, Faraday rotation due to Galactic or cosmologically intervening plasma that may be present along the sight-line to component D could not reasonably give rise to any rotation in the polarization position angle. The observed change in position angle for component D, $\Delta\theta = 32 \pm 7$ deg at $\lambda = 5300$ Å (for the F555W filter), would require a medium with a rotation measure of $RM = (2.0 \pm 0.4) \times 10^{12}$ radians m⁻²; however, for example, this is eight orders of magnitude larger than one of the highest values ever measured for an extragalactic radio source (e.g. 3C 295, Perley & Taylor 1991).

Consequently, we have argued that the ≈ 0.07 mag relative decrease in brightness of component D over the ≈ 100 day interval between March 1999 and June 1999 (Figure

⁸Interstellar polarization within the Milky Way is not significant for the Cloverleaf (e.g. Hutsemékers et al. 1998).

1) is evidence for microlensing of component D. In this scenario, component D evidently faded due to the motion of a microlens, causing it to be less magnified in June 1999. This is consistent with the earlier conclusions of Chae & Turnshek (1999, also §3.2), who interpreted the lower equivalent widths of the BELs in component D (observed with HST FOS in both June 1993 and December 1994) as evidence for microlens magnification of just the continuum of component D (not the BELs). Now, relying on the new results presented here, we can refine some of the conclusions of Chae & Turnshek (1999), and place better qualitative constraints on the size-scale of the polarized scattered-light region in relation to our understanding of the size-scales of the BEL and continuum-producing regions in QSOs.

We should point out that in all published individual spectra of the Cloverleaf components, the equivalent widths of the BELs in component D are smaller than observed in the other components. The first of four sets of component spectra were obtained in the spring of 1989 (Angonin et al. 1990) and this trend continues up until at least the spring of 2000, when HST-STIS spectra taken by Monier (PI) and several of the authors continued to show component D to have BELs with lower equivalent widths. This suggests that some level of microlens magnification of the continuum-producing region (but not the BELs) of component D is common over a relatively long time baseline.

The Cloverleaf’s macrolens by itself achromatically amplifies all light lying within $\approx 10^{19-20}$ cm of the central source into four point-like image components (see figure 1 of Chae & Turnshek 1999). Observations indicate that the macrolensed region includes the BEL region. This is consistent with expectations since the size of the region producing BELs like C IV and Ly α is estimated to be $\approx 10^{18} L_{46}^{0.5}$ cm from the central photoionizing source (Murray & Chaing 1998; Kaspi et al. 2000), where L_{46} is the lensed QSO luminosity in units of 10^{46} ergs s $^{-1}$. The source QSO luminosity in the Cloverleaf is not well-constrained because observations only provide results on the relative component amplifications; however,

the lens models suggest that the luminosity is likely to be of order L_{46} . Evidently the Cloverleaf is polarized because an asymmetric continuum scattering region also lies within the macrolensed region. The asymmetry is a requirement since the net polarization is non-zero. This region is not static; changes in parts of it must give rise to the variable continuum polarization which is seen. The fact that we have evidence for a variation in the net polarization over a ≈ 100 day interval in the observed frame (≈ 30 day interval in proper time) suggests that the size scales involved which lead to changes in polarization are $< 10^{17}$ cm. However, each part of this asymmetric scattering region by itself would be expected to give rise to highly-polarized continuum light ($p_{scatt,cont} > 10\%$), but when averaged over the entire asymmetric region there would be a much smaller net polarization.

For the purpose of illustration we note that if $\approx 80\%$ of the flux of component D was composed of the continuum plus BELs (as seen in the nearly identical spectra of components A, B and C), and the remaining $\approx 20\%$ of the flux of component D was solely composed of microlensed scattered continuum (i.e. no BEL flux), then the polarization of the scattered continuum component would have to be $p_{scatt,cont} \approx 13\%$ at $PA \approx 117$ deg to match the observations. This degree of polarization is reasonable for scattering.

Owing to the fact that the BEL equivalent widths in component D are observed to be smaller in comparison to the other components, the observed microlensed scattered-light region evidently does not scatter appreciable BEL flux. This suggests that the size-scale of the polarized scattered-light region (R_{scatt}) must be less than the size-scale of the region producing BELs, i.e., $R_{scatt} < 10^{18} L_{46}^{0.5}$ cm. At the same time, in order to produce the observed change in the polarization of component D relative to the other three components, the polarized scattered-light region must lie beyond the inner continuum-producing region which it reflects, far enough so that the inner continuum-producing region is not microlensed. This is because, if the entire scattering region were to lie within the microlensed region,

there would be a near constant magnification across the region during microlensing, the continuum light and scattered continuum light would be similarly amplified, and the polarization would remain unchanged among the four components during microlensing. Note that microlensing of an unpolarized central continuum-producing region (e.g. the continuum from the thermal accretion disk) is also not a possibility, since this would reduce the polarization in component D, which is not observed. These constraints are new; they were not addressed in the discussion of Chae & Turnshek (1999) because component polarization information was unavailable.

The size of the microlensed region on the source plane will be of order the Einstein ring size. Following Chae & Turnshek (1999), the Einstein ring size on the source plane produced by a microlensing star is given by $\eta_0 \approx 2 \times 10^{16} (M/M_\odot)^{0.5} h_{75}^{-0.5}$ cm, where M is the mass of the microlens. This is ≈ 8 light-days for a solar mass star, which is larger than the expected size of the continuum emitting region from any accretion disk. We would expect the size of the microlensed polarized scattering region to lie beyond this region.

Taken together our results therefore suggest that the size-scale of the polarized scattered-light region in the Cloverleaf is

$$2 \times 10^{16} (M/M_\odot)^{0.5} h_{75}^{-0.5} < R_{scatt} < 10^{18} L_{46}^{0.5} \text{ cm}. \quad (2)$$

From these results it is clear that a more rigorous future program dedicated to monitoring (photometric, spectroscopic, and polarimetric) the Cloverleaf would hold promise for providing valuable constraints on models of the inner regions of QSOs (i.e the BAL region, the BEL region, and the scattered-light region producing the polarization).

We are grateful for helpful communications throughout the course of this work from Drs. S. Casertano, J. Krist, P. Massey, E. Monier, and J. Walsh. We also thank Dr. S. Mao for helpful discussions regarding microlensing and comments on the manuscript.

REFERENCES

- Angonin, M.-C., Remy, M., Surdej, J., & Vanderriest, C. 1990, A&A, 233, L5
- Arnould, P., et al. 1993, in *Proceedings of the 31st Liege International Astrophysical Colloquium, Gravitational Lenses in the Universe*, eds. J. Surdej et al. (Liege: Univ. Liege, Inst. d’Astrophys), p169
- Belle, K. E., & Lewis, G. F. 2000, PASP, 112, 320
- Biretta, J., & McMaster, M. 1997, in *Instrument Science Report WFPC2 97-11* (STScI, Baltimore, MD)
- Chae, K.-H., & Turnshek, D. A. 1999, ApJ, 514, 587
- Fruchter, A. S., Hook, R. N., Busko, I. C., & Mutchler, M. 1997, in *1997 HST Calibration Workshop*, eds. S. Casertano et al. (STScI, Baltimore, MD) p518
- Fruchter, A. S., & Hook, R. N. 1998, astro-ph/9808087
- Goodrich, R. W., & Miller, J. S. 1995, ApJ, 448, L73
- Goodrich, R. W. 1997, ApJ, 474, 606
- Hutsemékers, D., Lamy, H., & Remy, M. 1998, A&A, 340, 371
- Kaspi, S., et al. 2000, ApJ, 533, 631
- Monier, E. M., Turnshek, D. A., & Lupie, O. L. 1998, ApJ, 496, 177
- Murray, N., & Chiang, J. 1998, ApJ, 494, 125
- Ogle, P. M. 1998, Ph.D. Thesis, Caltech
- Ostensen, R., et al. 1997, A&AS, 126, 393

- Perley, R. A., & Taylor, G. B. 1991, *AJ*, 101, 1623
- Press, W. H., Teukolsky, S. A., Vetterling, W. T., & Flannery, B. P. 1992, *Numerical Recipes in FORTRAN* (Cambridge University Press), p689
- Remy, M., Gosset, E., Hutsémekers, D., Revenaz, B., & Surdej, J. 1996, in *IAU Symp. 173, Astrophysical Applications of Gravitational Lensing*, eds. C. Kochanek & J. Hewitt (Dordrecht: Kluwer), p261
- Schmidt, G. D., & Hines, D. C. 1999, *ApJ*, 512, 125
- Turnshek, D. A. 1988, in *QSO Absorption Lines: Probing the Universe*, eds. J. C. Blades, D. Turnshek, & C. Norman (Cambridge University Press), p17
- Turnshek, D. A. 1995, in *QSO Absorption Lines, ESO Workshop*, ed. G. Meylan (Berlin: Springer), p317
- Turnshek, D. A., Lupie, O. L., Rao, S. M., Espey, B. R., & Sirola, C. J. 1997, *ApJ*, 485, 100
- Wardle, J. F. C., & Kronberg, P. P. 1974, *ApJ*, 194, 249
- Weymann, R. J., Morris, S. L., Foltz, C. B., & Hewett, P. C. 1991, *ApJ*, 373, 23

Table 1. WFPC2 Photometric and Polarimetric Observations

Observation Number	Exposure Time (sec)	Filter, Polarizer	PA_V3 (deg)	Relative Orient (deg)
15-16 Mar 1999				
1	8×40	F555W, none	57	N/A
2	8×40	F555W, none	98	N/A
3	8×40	F555W, none	100	N/A
4	1×70	F702W, none	57	N/A
5	2×70	F702W, none	98	N/A
6	1×70	F702W, none	100	N/A
7	8×100	F555W, POLQN18	98	14
8	8×100	F555W, POLQN18	100	16
9	8×100	F555W, POLQ	98	77
10	8×100	F555W, POLQP15	98	92
11	8×100	F555W, POLQN33	57	138
12	8×100	F555W, POLQN33	98	179
23-24 Jun 1999				
13	8×40	F555W, none	279	N/A
14	8×40	F555W, none	320	N/A
15	8×40	F555W, none	322	N/A
16	1×70	F702W, none	279	N/A
17	1×70	F702W, none	320	N/A
18	1×70	F702W, none	322	N/A
19	8×100	F555W, POLQN33	279	0
20	8×100	F555W, POLQN18	322	58
21	8×100	F555W, POLQ	320	119

Table 2a. Relative Magnitudes of the Cloverleaf Components at Two Epochs^a

Filter	Epoch	m_A	m_B	m_C	m_D
F555W	15-16 Mar 1999	0.000 ± 0.003	0.193 ± 0.003	0.300 ± 0.004	0.292 ± 0.003
	23-24 Jun 1999	-0.025 ± 0.003	0.188 ± 0.003	0.281 ± 0.004	0.368 ± 0.003
F702W	15-16 Mar 1999	0.000 ± 0.007	0.171 ± 0.007	0.320 ± 0.008	0.385 ± 0.008
	23-24 Jun 1999	-0.004 ± 0.008	0.163 ± 0.008	0.344 ± 0.009	0.446 ± 0.009

^a The magnitude of component A is set to zero for the March epoch.

Table 2b. Relative Magnitude Changes of the Components Over 100 Days

Filter	Δm_A	Δm_B	Δm_C	Δm_D
F555W	-0.025 ± 0.004	-0.005 ± 0.004	-0.019 ± 0.006	0.076 ± 0.004
F702W	-0.004 ± 0.011	-0.008 ± 0.011	0.024 ± 0.012	0.061 ± 0.012
F555W+F702W ^a	-0.023 ± 0.004	-0.005 ± 0.004	-0.010 ± 0.005	0.074 ± 0.004

^a The Δm listed is the variance-weighted mean of the F555W and F702W results.

Table 3. F555W Relative Polarimetric Results for the Cloverleaf Components^a

Parameter	A	B	C	D	\overline{ABC}^b
15-16 Mar 1999					
q (%)	-1.35 ± 0.43	-1.42 ± 0.46	-1.42 ± 0.46	-2.65 ± 0.47	-1.39 ± 0.26
u (%)	0.78 ± 0.49	1.76 ± 0.52	1.10 ± 0.53	-1.13 ± 0.53	1.19 ± 0.30
p (%)	1.56 ± 0.45	2.27 ± 0.50	1.79 ± 0.49	2.88 ± 0.48	1.83 ± 0.28
p_{corr} (%) ^c	1.49	2.21	1.72	2.84	1.81
PA (deg) ^c	75.0 ± 8.8	64.5 ± 6.1	71.0 ± 8.0	101.5 ± 5.2	69.7 ± 4.4
$\Delta q_{D,\overline{ABC}}$ (%)	—	—	—	-1.26 ± 0.54	$\equiv 0$
$\Delta u_{D,\overline{ABC}}$ (%)	—	—	—	-2.32 ± 0.61	$\equiv 0$
23-24 Jun 1999					
q (%)	—	—	—	-0.91 ± 0.61	-0.88 ± 0.34
u (%)	—	—	—	-0.43 ± 0.62	0.11 ± 0.35
p (%)	—	—	—	1.00 ± 0.61	0.89 ± 0.34
p_{corr} (%) ^c	—	—	—	0.79	0.82
PA (deg) ^c	—	—	—	103 ± 18	87 ± 11
$\Delta q_{D,\overline{ABC}}$ (%)	—	—	—	-0.03 ± 0.70	$\equiv 0$
$\Delta u_{D,\overline{ABC}}$ (%)	—	—	—	-0.54 ± 0.71	$\equiv 0$

^a Quoted errors are relative statistical errors.

^b The combined result of components A, B, and C.

^c We use the formula of Wardle & Kronberg (1974) to correct the bias toward higher polarization degree in low S/N ratio data:

$$p_{\text{corr}} = p \left[1 - \left(\frac{\sigma_p}{p} \right)^2 \right]^{1/2}.$$

Our derived errors in PA are in good agreement with their general prescription for estimating the PA errors under such conditions: $\sigma_{PA} \approx 28.65\sigma_p/p$ deg.

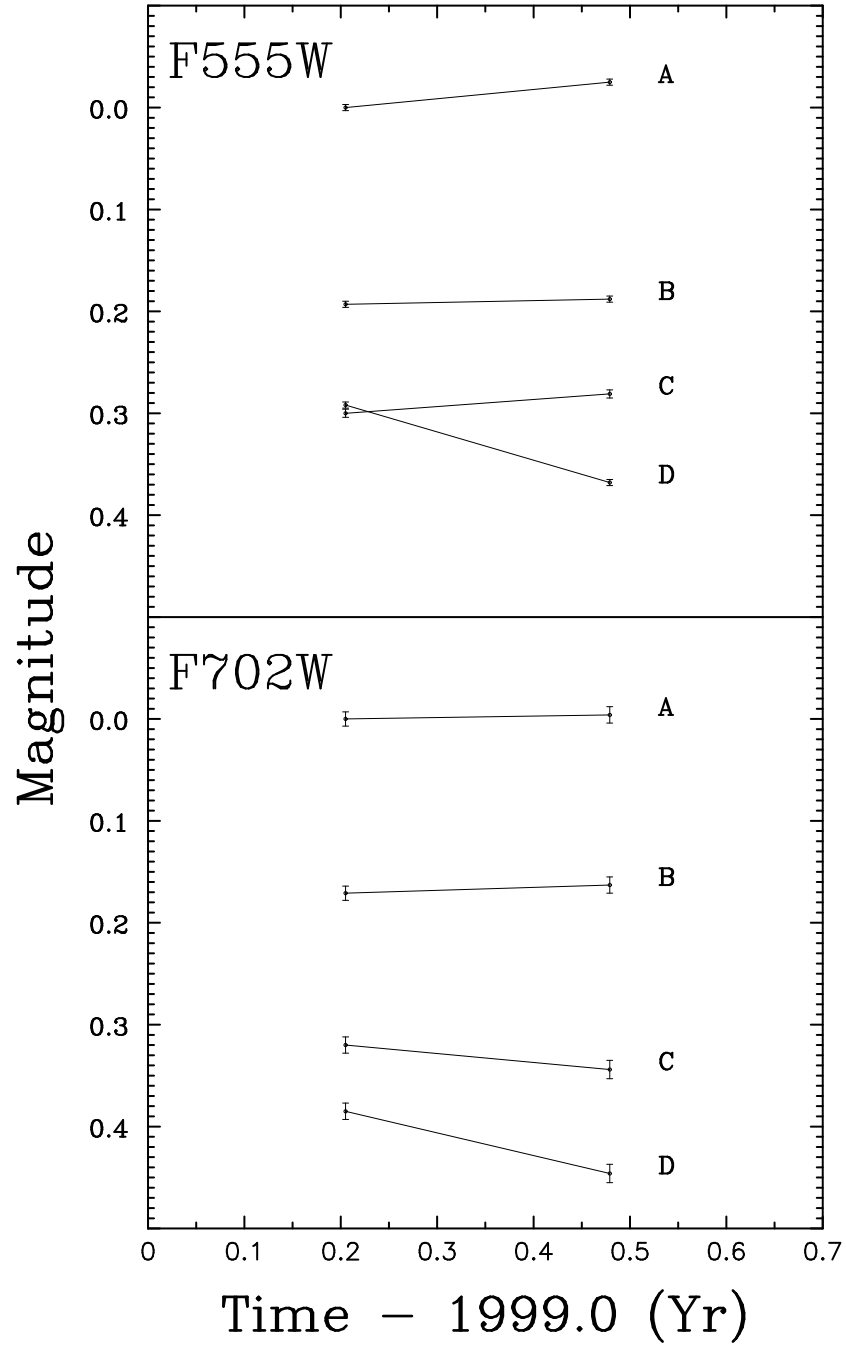


Fig. 1.— HST WFPC2 F555W and F702W brightnesses of Cloverleaf components B, C, and D relative to component A in March 1999.

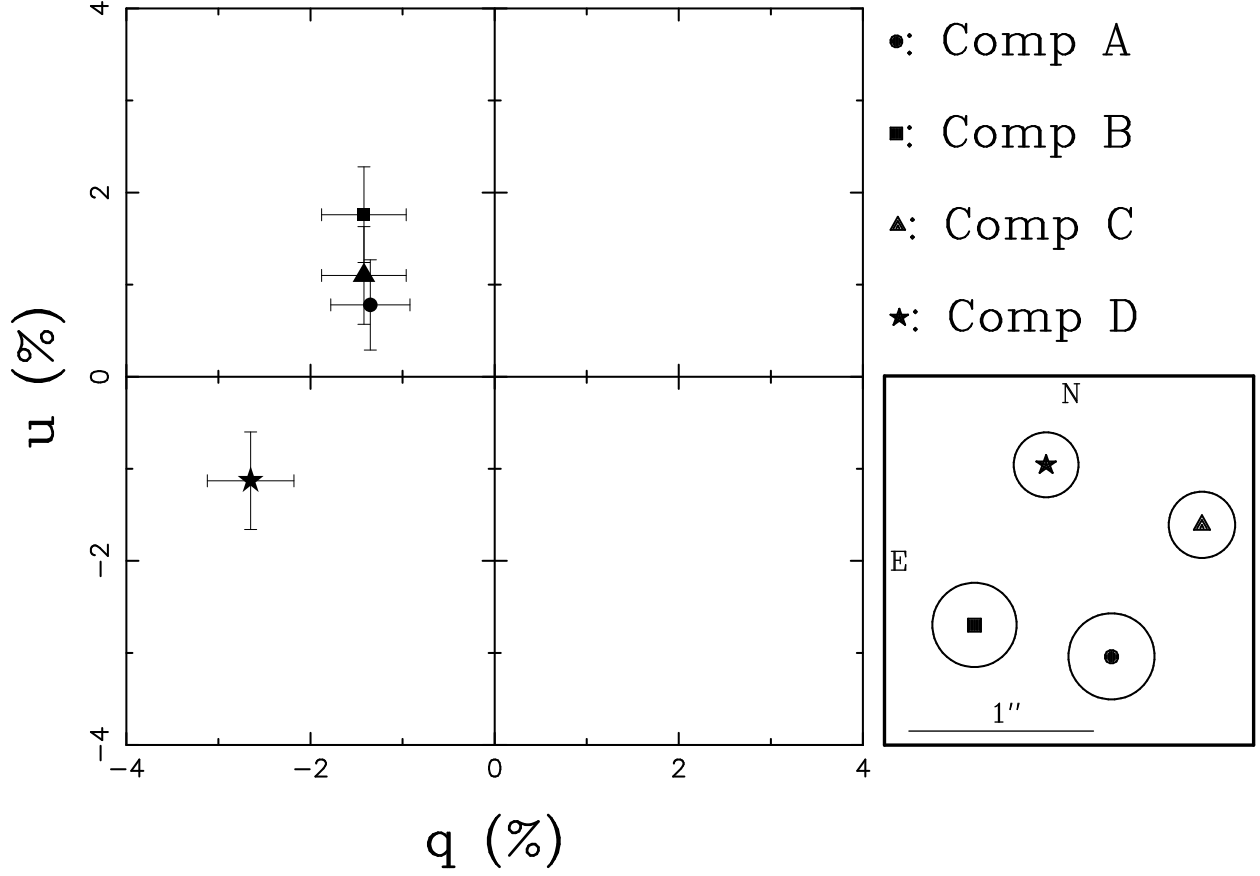


Fig. 2.— Stokes parameters derived from the March 1999 HST WFPC2 F555W observations of the four components of the Cloverleaf. The legend on the upper right specifies the component designations (A, B, C, D). The box on the lower right shows the relative spatial location of the components; the size of the circles drawn around the components is proportional to their relative brightnesses. The June 1999 observations were less reliable (§2), and for this reason they are not shown here but are only reported in Table 3.